# Low-temperature electron transport in Si with an MBE-grown Sb $\delta$ layer

S. Agan,* O. A. Mironov,† E. H. C. Parker, and T. E. Whall
*Department of Physics, University of Warwick, Coventry CV4 7AL, United Kingdom*

C. P. Parry
*Institut fuer Halbleitertechnik, Universitaet Stuttgart, D 70569 Stuttgart, Germany*

V. Yu. Kashirin, Yu. F. Komnik, and Vit. B. Krasovitsky
*B. Verkin Institute for Low Temperature Physics and Engineering, National Academy of Sciences of Ukraine, 310164 Kharkov, Ukraine*

C. J. Emeleus
*Department of Physics and Astronomy, University of Glasgow, Glasgow, G12 8QQ, United Kingdom*
(Received 23 June 1999; revised manuscript received 27 December 1999; published 23 January 2001)

Studies of the electrical properties of Si single crystals with $\delta$(Sb) layers of various sheet densities $N_D$, of Sb atoms ($5\times10^{12}$–$3\times10^{14}\,\mathrm{cm}^{-2}$) have furnished detailed information about the low-temperature features of the electron transport in this system. The metal-type conductivity of $\delta$ layers at $N_D\geqslant3\times10^{13}\,\mathrm{cm}^{-2}$ exhibits manifestations of the weak localization of electrons and electron-electron interaction in a two-dimensional system. The temperature dependence of electron phase relaxation time, the spin-orbit interaction time, and parameter $\lambda^D$ of the electron-electron interaction are determined. It is found that a decrease in the electron density in the $\delta$ layer is accompanied by decrease in the parameter $\lambda^D$. The effect of electron heating by an electric field is used to find the temperature dependence of the electron-phonon relaxation time. At low temperature the hopping-type conductivity of $\delta$ layers at $N_D\leqslant1\times10^{13}\,\mathrm{cm}^{-2}$ is realized; at sufficiently low temperatures (<10 K) the two-dimensional Mott law of variable-range hopping is seen. The nonlinearity of the current-voltage characteristics observed is well described by the theory of non-Ohmic hopping conductivity in moderately strong electric fields.

DOI: 10.1103/PhysRevB.63.075402 PACS number(s): 73.20.Fz, 81.15.Hi

## I. INTRODUCTION

The $\delta$ layer is a conducting layer of atomic thickness, which is formed in a pure semiconducting crystal matrix due to impurity atoms located within one crystallographic plane. The conduction electrons in a semiconductor with a $\delta$ layer are in a symmetric V-shaped potential well, formed by screening of the potential of impurity atoms by electrons.[1] The electrons in the potential well form a two-dimensional electron gas in the plane of the $\delta$ layer, and behave as free particles. The states are, however, quantized in the direction perpendicular to the plane of the layer. The number of size-quantized subbands and their filling are determined by the sheet density of impurity atoms. Usually only a few subbands are filled, and the mobilities of charge carriers are strongly dependent on the number of the subband. The filling of the subband and the mobilities of charge carriers were the object of initial studies of $\delta$ layers [mainly of $\delta$(Si) layers in GaAs].[2–8]

The transport mobility of the electrons is lower in $\delta$ layers than in modulation-doped heterojunctions because impurity scattering is determined by the same impurity atoms which formed the $\delta$ layer. However, $\delta$ layers are distinguished by an important and valuable feature: they allow an arbitrary density of two-dimensional electrons at very low sheet density values ($\approx10^9-10^{10}\,\mathrm{cm}^{-2}$), for which the conductivity in the $\delta$ layer is of ''hopping'' type, to very high values ($\approx10^{14}\,\mathrm{cm}^{-2}$), for which metallic conductivity is realized. This feature of $\delta$ layers provides a unique opportunity to study the effect of the concentration of two-dimensional electrons on the relaxation and interaction of electrons in a two-dimensional electron gas, and on the character of the transition from the metallic to hopping conductivity. For $\delta$(Sb) layers in silicon this transition occurs in the range from 0.01 ML of Sb atoms to 0.05 ML in the $\delta$ layer, which corresponds to electron densities from $6.7\times10^{12}$ to $3.35\times10^{13}\,\mathrm{cm}^{-2}$.[9]

## II. SAMPLE DETAILS AND MEASURING TECHNIQUES

The Sb $\delta$ layers were prepared by low-temperature silicon molecular-beam epitaxy on Si(100) substrates. Growth at 250 °C, and below, avoids Sb profile smearing by surface segregation.[10] The configuration of the impurity region meets the requirements of galvanomagnetic measurement (a narrow strip with current and potential leads forming contact areas on the crystal surface). The results of measurements on the five samples investigated—the preassigned concentration $N_D$ of impurity Sb atoms, the resistance $R_\square$, and the Hall concentration $n$ of mobile charge carriers at 4.2 K—are given in Table I. According to precision x-ray diffractometry, the ''structural'' thickness of the $\delta$(Sb) layers at $N_D=2\times10^{14}\,\mathrm{cm}^{-2}$ is below 20 Å.[11] A similar result was obtained from secondary-ion-mass spectrometry and transmission electron microscopy.[12]

The galvanomagnetic properties (resistance, magnetoresistance, Hall effect) were measured in the temperature range 1.6–300 K in a constant current typically $10^{-8}$ A for high-

 ©2001 The American Physical Society

TABLE I.

| Parameter | Samples | | | | |
|---|---|---|---|---|---|
| | A | B | C | D | E |
| $N_D$, $cm^{-2}$ | $3\times10^{14}$ | $1\times10^{14}$ | $3\times10^{13}$ | $1\times10^{13}$ | $5\times10^{12}$ |
| $N_D^{-1/2}$. Å | 5.7 | 10 | 18 | 32 | 45 |
| $R_\square^{4.2}$, Ω (at 4.2 K) | $1.17\times10^3$ | $1.53\times10^3$ | $4.81\times10^3$ | $10^9$ (at 8 K) | $2\times10^{11}$ (at 8 K) |
| $n$, $cm^{-2}$ (at 4.2 K) | $9.5\times10^{13}$ | $7.8\times10^{13}$ | $3.1\times10^{13}$ | - | - |
| $\varepsilon_1$, meV | 42 | 41 | 37 | 44 | 44 |
| $\lambda_T^D$ | 0.93 | 0.90 | 0.60 | - | - |
| $F$ | 0.093 | 0.133 | 0.53 | - | - |

Ohmic samples, and $10^{-6}$–$10^{-5}$ A for low-Ohmic samples. At 4.2 K and below, the sample was immersed in liquid helium; the accuracy of temperature stabilization in this region was 0.01 K. At higher temperatures, the sample was immersed in the helium vapor, and the temperature was maintained constant to within 0.02 K. The magnetic field was generated within a superconducting magnet (up to 5.0 T) or a resistive electromagnet (up to 2.0 T).

## III. GENERAL PICTURE OF CHANGES IN KINETIC CHARACTERISTICS

### A. Preliminary comments

At low temperatures (~4 K), the conductivity of samples with the $\delta$ layer is dictated by the conductivity of the $\delta$ layer, i.e., by the electrons occupying the quantum states (subbands) in the potential well rather than by electrons elsewhere in the surrounding Si. The theory of $\delta$ layers was developed in Refs. 13 and 14. Numerical calculations were performed in Refs. 2, 6, and 15–18 for GaAs-based structures and in Ref. 19 for the $\delta$(B) layer in Si. It is known that the isoenergetic surfaces in the conduction band of Si are anisotropic. The electrons of the conduction band form six rotation ellipsoids along the axes ⟨100⟩. The effective masses corresponding to the directions along the long ellipsoid axis and across are $m_L=0.916m_0$ (longitudinal mass) and $m_t=0.19m_0$ (transverse mass), $m_0$ is the free-electron mass. In the quantum well in the (100) plane of Si, subbands are formed, which have longitudinal mass and degeneracy multiplicity $g_v=2$ and a transverse mass and degeneracy multiplicity $g_v=4$. As a result, the number of subbands in the well is different for each group. According to our estimates, in the sequence of the samples studied—A, B, C, D, and E—the number of subbands decreases from 5–9 to 2–4 (for the longitudinal and transverse masses, respectively). We did not perform a numerical calculation of the subband energies, similar to that made in Refs. 20 and 21 for inversion layers, because we do not know exactly the potential well shape of the $\delta$ layer. In addition, such a calculation is not topical for $\delta$ layers. The nature of $\delta$ layers is such that the impurity atoms responsible for the formation of a quantum potential well are themselves factors provoking strong impurity scattering. The estimated disorder parameters $k_F l$ for samples A, B, and C are quite low (5–20). The strong intervalley scattering leads to smearing of the subbands. As shown below, the elastic relaxation time in the samples studied is $3\times10^{-15}$ s and shorter, which corresponds to the smearing of the level about 200 meV. This is comparable with the expected energy difference for the subbands.

The electron gas in the quantum well formed by the $\delta$ layer should be regarded as two dimensional. While describing the conductivity of this electron gas, it is necessary to use the ''drift'' effective mass $m$, which is an average value of longitudinal and transverse masses: for three-dimensional (3D) electron gas, $m=3m_1m_t/2m_1+m_t$, and for 2D electron gas, $m=2m_1m_t/m_1+m_t$. We used a value that was calculated for 2D electron gas for orientation (100) Si, $m=0.315m_0$.[20]

The filling of subbands and the carrier mobilities in them change considerably with the number of the subband. The density of states is nearly the same in two-dimensional subbands, and is equal to $\nu=m/\pi\hbar^2$, but the carrier concentration in the subbands is dependent on the energy: $n_i=m\varepsilon_i/\pi\hbar^2$ ($\Sigma n_i=n$, where $n$ is the total carrier concentration). Thus the partial carrier concentration in the subbands decreases when the number of the subband increases.

The partial carrier mobility in the subbands changes under the influence of at least two competitive factors. On the one hand, the increasing number of the subband, and the decrease in $|\varepsilon_i|$, should enhance the efficiency of the impurity–caused scattering due to a decrease in the momentum and the Fermi velocity of the electrons, i.e., their mobility should decrease. On the other hand, an increasing number of the subband broadens the region of electron localization, which enhances the carrier mobility. The latter factor turns out to predominate; calculation[14,16–18] shows that the partial mobility of carriers increases with the number of the subband. Similar results follow from experimental findings.[4,5,7,22,23]

The total conductivity is a sum of the conductivities of the occupied subbands. These conductivities are nearly similar because when the number of the subband increases, the concentration of the carriers decreases though their mobility grows. This is supported by the fact that in the region of the metal-type conductivity (beyond the metal-insulator transition) the conductivity changes practically linearly with the carrier concentration, i.e., with the number (sum) of subbands.[14] The total conductivity of the $\delta$ layer can be described with a certain mobility $\mu$ and diffusion coefficient $D$, which are used below.

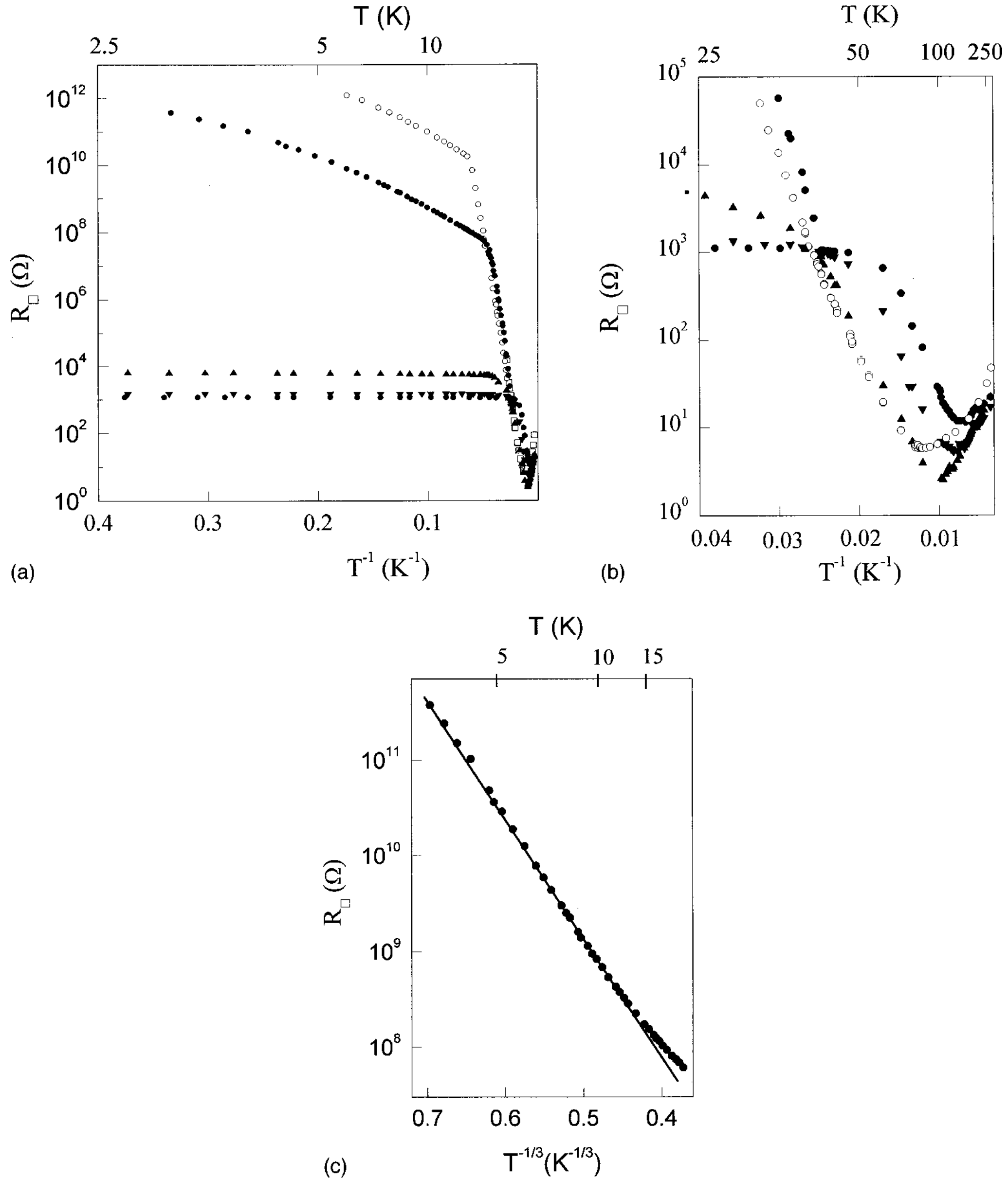


FIG. 1. $R(T)$ dependencies for samples A (1), B (2), C (3), D (4), and E (5). The general picture of resistance variations is shown in the low-temperature region in the $\ln R_\square - T^{-1}$ coordinates (a), at intermediate temperatures (b), and in the resistance variation of sample D in the low-temperature region in the $\ln R_\square - T^{-1/3}$ coordinates (c).

While describing conductivity and quantum corrections to conductivity which are related to weak localization (WL) and electron interaction (EEI), we may assume that the system behaves as if it should contain one ''effective'' subband. A similar conclusion is reached for multivalley systems if the rate of intervalley scattering is high enough. The form of the WL corrections was analyzed for a two-subband system.[24] It was shown that under strong intersubband scattering ($1/\tau_v \gg 1/\tau_\varphi$, $\tau_\varphi$ is the phase relaxation time) the corrections do not change functionally, and the influence of many subbands reduces to renormalization of the diffusion coefficient.

Now we consider the experimental results describing the changes of the kinetic characteristics of the samples in a wide temperature range. It will be shown below that the conductivity is essentially influenced not only by the electrons of the $\delta$ layer, but also by the electrons activated to the Si conduction band.

### B. Temperature variation of resistance

Figure 1 shows the temperature dependences of the resistance, $R(T)$, taken on the samples studied. In the low-temperature region, samples A, B, and C display a very weak increase in resistance as the temperature decreases [Fig. 1(a)]. We show that the change is due to the interference effects of weak localization of electrons and the electron-electron interaction (see Sec. IV). For samples D and E, the low-temperature change in the resistance is determined by the mechanism of hopping conductivity, which we shall discuss later on. As the temperature rises, the dependencies

$R(T)$ change for all samples: the resistance decreases sharply with increasing temperature [Fig. 1(b)]. In the samples with lower resistance, the transition temperature $T^*$ rises (e.g., for sample E the typical value of $T^*$ is ~16 K; for samples D, B, C, and A, it is about 25, 35, 50, and 60 K, respectively). Variations of the resistance above these temperatures are described well by

$$R=R_1 \exp(\varepsilon_1/kT). \tag{1}$$

The dependence suggests that in this region conductivity is controlled by the activation of the impurity carriers. The estimated values of activation energy $\varepsilon_1$ are given in Table I: they are close to the known binding energies for donor states of the Sb impurity in silicon [e.g., 42.7 meV (Ref. 21)]. As the temperature goes above the region described by Eq. (1), the dependence $R(T)$ changes: the resistance has a minimum and then grows weakly [Fig. 1(b)]. The growth is due to scattering of the activated electrons by acoustic phonons under the condition of depletion of donor centers.

Thus, at high temperatures there is a competition between the conduction of the $\delta$ layer and electrons in the conduction band, which are in thermal equilibrium with the electrons at the donor centers. The band conduction channel is apparently much wider than the geometric thickness of the $\delta$ layer. A distinguishing feature of the objects under investigation is that impurity atoms are spatially localized in the same crystalline plane along which electron transport occurs in the $\delta$ layer. The conductivity of the $\delta$-layer itself is determined by the overlapping wave function tails of the electrons localized at impurities. Table I contains the values of $N_D^{-1/2}$ (Å) characterizing the mean distance between the ionized Sb atoms in the $\delta$ layer. These values can be compared with the Bohr radius, $a_B=\hbar\varepsilon^*/me^2$ (where $e$ is electron charge; $\varepsilon^*$ is static dielectric constant, equal to 11 for Si), characterizing the size of the electron wave function at an impurity atom. For Sb in the Si matrix, $a_B \approx 23$ Å. The radius of the state $a=\hbar/(2m\varepsilon_1)^{1/2}$ has approximately the same value. These estimates and the data in Table I show that because of the overlapping of the electron wave functions at impurities in samples A, B, and C, the conductivity of the $\delta$ layer is realized in the impurity band and it may be regarded as a two-dimensional system with metallic conductivity.

Since the tails of the electron wave functions overlap only slightly in samples D and E, the low-temperature conductivity of the $\delta$ layer is of the hopping type. It is known that under certain conditions electrons can hop from one impurity atom to another by thermally activated tunneling, without a transition to the conduction band. Although the mobility of the electrons hopping over the impurity levels is quite small, because it is influenced by the interaction of widely separated impurities, at low temperatures the conduction through impurities becomes dominant due to the ''freezing out'' of electrons in the conduction band. The resulting specific electric conductivity is[25]

$$\rho^{-1}(T)=\rho_1^{-1}\exp(-\varepsilon_1/kT)+\rho_3^{-1}\exp(-\varepsilon_3/kT), \tag{2}$$

where the first term describes the band conductivity, and the second term corresponds to the hopping-type conductivity with the activation energy constant $\varepsilon_3$. The latter term has its origin from the scatter of impurity energy levels: the transition of an electron from one impurity atom to another is possible when phonons are absorbed or emitted. It is seen in Fig. 1(a) that at lowering temperature the dependence Eq. (1) with the activation energy $\varepsilon_1$ changes for samples D and E. A temperature region appears in which the second term of Eq. (2) with low activation energy $\varepsilon_3$ becomes dominant. As follows from experimental results, it is equal to 3.9 meV. This exponential dependence is evident to ~10 K.

After further decreases in temperature, the dependence deviates from the above exponential behavior due to hopping-type conductivity with a varying length of the jump (variable range hopping).[25] At very low temperatures the hopping conductivity is characterized mainly by states with energies within a narrow band near the Fermi level, and the width of this band decreases with lowering temperature. The states within this band are farther apart, the length of the jumps increases as $T^{-1/4}$ and the activation energy decreases as $T^{3/4}$. The temperature dependence of the specific resistance takes the form (Mott's law):[26]

$$\rho(T)=\rho_0 \exp(T_0/T)^{1/4}, \tag{3}$$

where $T_0=\beta/k\nu(\mu)a^3$, $\nu(\mu)$ is the density of states at the Fermi level, and $\beta=21.2$ (Refs. 25 and 27) is a numerical coefficient. For a two-dimensional system, Mott's law variable range hopping is[28]

$$\rho(T)=\rho_0' \exp(T_0'/T)^{1/3}, \tag{4}$$

where $T_0'=\beta'/kg'(\mu)a^2$, $g'(\mu)$ is the two-dimensional density of states at the Fermi level, and $\beta'=13.8$.[27]

The analysis of experimental results for sample D shows that below 11 K the experimental points fall well on a straight line in $\ln R - T^{-1/3}$ coordinates [Fig. 1(c)]. (Note that in the $\ln R \sim T^{-1/4}$ coordinates, the fit to a straight line is not as good.) Thus in sample D a decrease in the temperature leads first to hopping-type conductivity with a constant activation energy, and then to variable-range hopping conductivity. [The hopping-type electron transport was earlier observed in the $\delta\langle$Sb$\rangle$ layers of GaAs (Refs. 29 and 30).]

Hopping-type conductivity with a constant activation energy $\varepsilon_3$ is realized when the following inequality is obeyed:[25]

$$\varepsilon_3/kT \leqslant 2r/a, \tag{5}$$

where $r$ is the mean distance between the impurity centers. Putting $r=N_D^{-1/2}$, $\varepsilon_3=3.9$ meV, and $a\approx 19$ Å, we can use Eq. (5) to estimate the temperature at which the conduction can change to the type described by Eq. (4). For sample D, the left- and right-hand sides of Eq. (5) become equal at $T=13$ K, which agrees well with the experimental value of $\approx 11$ K.

The analysis of the low-temperature conduction of the samples investigated and the dependence of the resistance $R_\square$ on the Sb atom density in the $\delta$ layer (see Table I) shows that the metal-insulator transition (MIT) occurs at $N_D \leqslant 3\times 10^{13}$ cm$^{-2}$: samples A, B, and C are on the metallic side of the transition, and samples D and E are on the insulator side.

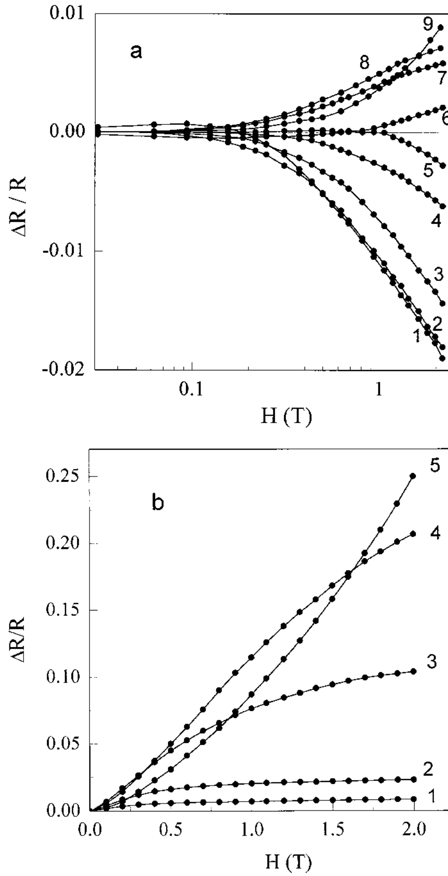


FIG. 2. Magnetic-field dependencies of resistance of samples A (a) and D (b) at various temperatures K: 1.64 (1), 4.2 (2), 8 (3), 19 (4), 22.7 (5), 26 (6), 28.1 (7), 40.5 (8), and 44 (9) (a); and 18.8 (1), 20.4 (2), 23.15 (3), 25.25 (4), and 27.25 (5) (b).

This agrees with the results in Ref. 9, which shows that the MIT takes place in the range 0.01–0.05 ML of Sb atoms in the $\delta$ layer. The metal-insulator transition was earlier observed on Si samples with a $\delta$ layer of boron, which is an acceptor impurity.[19] In that case the MIT occurs at $N_A \sim 1.10^{13}\,\mathrm{cm}^{-2}$.

### C. Magnetoresistance

In the samples studied the magnetic field variation of the resistance $\Delta R/R$ [where $\Delta R = R(H) - R(0)$], has different signs and very different amplitudes in different temperature regions. At low temperatures (much below the characteristic temperature $T^*$, above which the electrons are activated to the conduction band), the magnetoresistance (MR) is negative for samples A, B, and C [Fig. 2(a)] due to the quantum WL-induced correction to conductivity. As the temperature is increased, the amplitude of the negative MR decreases appreciably. At the lowest temperatures ($T<3$ K) sample *A* has a magnetic-field region in which the MR is positive, but as the magnetic field increases, the MR becomes negative. The features of negative MR under the condition of the WL effect are discussed in Sec. IV. At transient temperatures near $T^*$ the MR of samples A, B, and C is positive; it first increases in amplitude and the curve saturates in MR, then decreases at $T>T^*$.

For samples D and E, the magnetoresistance is positive in the region of the hopping-type conductivity, but its value is rather low and vanishes below 17 K. This behavior is at variance with theoretical ideas of magnetoresistance of semiconductors with the hopping-type conductivity.[31,32] According to Ref. 31, a high magnetic field squeezes the wave functions of the impurity electrons laterally, and the overlapping of the exponential tails of the electron wave functions at the neighboring impurities decreases. As a result, the magnetic field can cause an exponential increase in the magnetoresistance. However, an important feature of the objects under investigation is that the impurity atoms, through which hopping occurs, form a two-dimensional system. In a two-dimensional network, of special importance are the key elements responsible for the most ''difficult'' jump. In this case the overlapping of the electron wave functions at the nearest impurities in the magnetic field is less important than the contribution of the key elements of the network, which do not seem to change their properties in the magnetic field. Note that the distribution of the key elements determines a certain characteristic size of the critical subnetwork $L_0$. The knowledge of this parameter is very important when it is necessary to describe the nonlinearity of current-voltage curves under the condition of the hopping-type conductivity in moderate electric fields (see Sec. VI).

In the transient interval of temperatures near $T^*$ the MR of samples D and E increases exponentially [Fig. 2(b)]. In the interval 18–30 K and at 16 kOe, $\Delta R/R$ increases by two orders of magnitude. In the temperature region where the electrons are activated to the conduction band, the MR decreases exponentially as $1/T$, reproducing the behavior of zero-field resistance. At these transient temperatures the $\Delta R/R(H)$ dependencies have the form of saturation curves. Then in a progressively increasing interval of magnetic fields an initial portion reappears which can be approximated by the ordinary dependence $\Delta R/R \propto H^n$, where $n \sim 1.5-2$. The saturation of the MR suggests two conducting channels in the transition interval of temperatures: the conductivity of the $\delta$ layer itself and the band conductivity. For simplicity, we shall term the latter channel a λ region, since the carriers behave as free electrons. Since the $\delta$ layer is slightly influenced by the magnetic field but the λ regions are more strongly affected, it is easy to prove that if $R^{\lambda}(0) < R^{\delta}$ at some temperature and $R^{\lambda}(H) > R^{\delta}$ in a strong magnetic field, the dependence $R(H)$ will tend to a constant value determined by $R^{\delta}$ since $R^{-1} = (R^{\delta})^{-1} + (R^{\lambda})^{-1}$. The magnetoresistance saturation thus corresponds to the concept used to discuss the resistance behavior of the samples in the transient and activation intervals of temperature.

### D. Hall effect

For samples A, B, and C, the Hall voltage $V_H$ varies linearly in the studied interval of magnetic fields both at low and high temperatures. The linearity of the Hall voltage at low temperatures when the sample conductivity is dependent only on the conductivity of the $\delta$ layer is the evidence supporting the validity of the concept of the conventionally single effective subband. Indeed, if the Hall voltage were

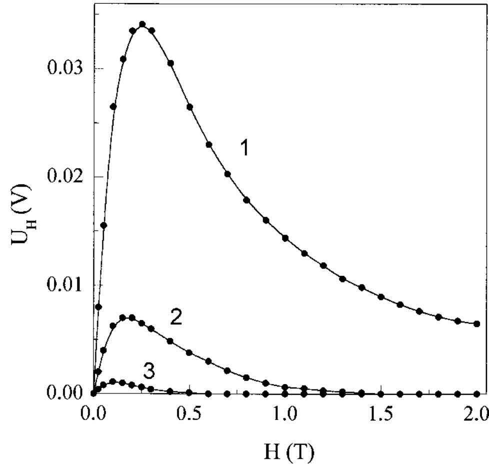


FIG. 3. Magnetic-field variations of the Hall voltage for sample D at different temperatures K: 20.4 (1), 18.8 (2), and 17.5 (3).

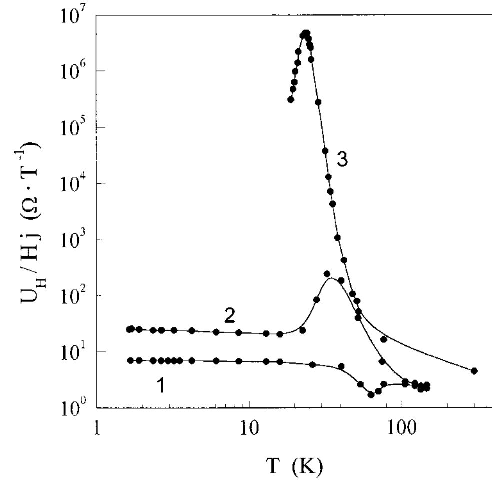


FIG. 4. Dependencies of the reduced Hall voltage $U_H/Hj$ ($j$ is the current through the sample) upon temperatures for samples A (1), C (2), and D (3).

influenced by subbands considerably different in carrier mobilities and concentrations, the Hall effect could not be linear. In the transient region near $T^*$, corresponding to the onset of the electron activation to the Si conductivity band, the dependence $V_H(H)$ starts to display weak nonlinearity, which is due to two conductivity channels operating in the transient region. We shall describe the Hall emf with the reduced value $V_H/Hj$ ($j$ is the current through the sample). The Hall concentration obtained for samples A, B, and C at low temperatures agrees well with the sheet density $N_D$ of Sb impurity atoms preassigned during preparation of the samples (see Table I). In the region of the activation-type band conductivity, the $V_H/Hj$ value decreases with rising temperature by the exponential dependence on $1/T$ (as the resistance does), which accounts for an increasing number of electrons activated into the conduction band. At low temperatures, $V_H/Hj$ of samples A, B, and C increases slightly parallel with the resistance, as the temperature goes down, which is the manifestation of the WL and EEI effects.

At low temperatures the Hall mobility $\mu_H = R_{\square}^{-1} V_H/H_i$ is quite small in samples A, B, and C (10–20 $\mathrm{cm^2\,V^{-1}\,s^{-1}}$); the mobility of the electrons activated to the Si conductivity band, i.e., at $T \gg T^*$, appears to be high ($\sim 10^3 - 10^4\,\mathrm{cm^2\,V^{-1}\,s^{-1}}$).

For samples $D$ and $E$, the Hall voltage below 17 K becomes negligibly small, and at the beginning of the transient region the curves $V_H(H)$ look anomalous: they have a maximum and then decrease asymptotically (Fig. 3). If we determine the Hall concentration from the initial quasilinear part of the $V_H(H)$ dependence, the result appears to be much lower than $N_D$ (e.g., the Hall concentration found from the curves in Fig. 3 is $10^9\,\mathrm{cm^{-2}}$, while $N_D \approx 10^{13}\,\mathrm{cm^{-2}}$). We can hardly explain this anomaly unambiguously. We should remember that it appears when activated carriers come to the conductivity band, and these carriers are more mobile than the carriers in the subbands.

At high temperatures the distinct linear dependence $V_H(H)$ observed for sample D and E (and for samples A, B, and C) permit quite a reliable estimation of the concentration of the electrons activated to the conductivity band. At 200–300 K the following electron concentrations are obtained from the Hall voltage: $3\times10^{14}\,\mathrm{cm^{-2}}$ for samples A, B, and C, and $\approx 1.5\times10^{14}\,\mathrm{cm^{-2}}$ for samples D and E. At high temperatures the electron concentration is practically similar for different samples, while the low-temperature concentrations differ by several orders of magnitude.

In the transient interval of temperatures for samples D and E, as well as for sample C, the temperature dependence of $V_H/Hj$ exhibits a sharp maximum (Fig. 4). Its existence and symmetrical form suggest the presence of two groups of electrons with considerably different mobilities: the conduction-band electrons, whose density is exponentially dependent on temperature, and the impurity band electrons with low (e.g., hopping type) mobility (the existence of a symmetrical maximum in the temperature dependencies of the Hall coefficient under this condition was proved in Ref. 25). The behavior of the Hall voltage for samples D and E demonstrates visually the transition from hopping-type conductivity to band conductivity with increasing temperature.

## IV. INTERFERENCE EFFECTS IN THE CASE OF METAL-TYPE CONDUCTIVITY

The metallic conductivity of $\delta$ layers (samples A, B, and C) exhibits manifestations of WL (Refs. 33 and 34) and EE (Refs. 35–41) effects. These effects occur in disordered systems under the condition of strong elastic scattering of electrons: they arise from interference, and require in quantum corrections to the conductivity, which results in the resistance being dependent on both temperature and magnetic field. Analysis of this behavior yields information about electron relaxation and interaction within the system under investigation: the time of phase breaking of the electron wave function, $\tau_\varphi$, and its temperature variation, the time of spin-orbit interaction (SOI) $\tau_{SO}$ during elastic scattering of electrons by impurities and the characteristic constants of the electron-electron interaction λ.[39–41]

In a two-dimensional system the contribution of the WL effect to the temperature dependence of conductivity in zero

magnetic field can be described as:[34,36,40]

$$\Delta\sigma_T^L = -\frac{e^2}{2\pi^2\hbar}\left[\frac{3}{2}\ln\frac{\tau_\varphi^*}{\tau} - \frac{1}{2}\ln\frac{\tau_\varphi}{\tau}\right], \tag{6}$$

where $\tau$ is the time of the elastic electron relaxation, $\tau_\varphi^{-1} = \tau_{\varphi 0}^{-1} + 2\tau_s^{-1}$, $(\tau_\varphi^*)^{-1} = \tau_{\varphi 0}^{-1} + \frac{4}{3}\tau_{so}^{-1} + \frac{2}{3}\tau_s^{-1}$, $\tau_{\varphi 0}$ is the time of phase relaxation due to inelastic scattering, and $\tau_s$ is the time of spin-spin scattering by magnetic impurities (when impurities are absent, as in our case, this time is very large and may be disregarded). The common practice is to use the representation $\tau_\varphi^{-1} \propto T^p$, where $p$ is the exponent dependent on the mechanism of inelastic relaxation. At lowering temperature the correction [Eq. (6)] makes the resistance increase when SOI is weak ($\tau_{so} \gg \tau_{\varphi 0}$) and decrease when SOI is strong ($\tau_{so} \ll \tau_{\varphi 0}$).

The temperature dependence of the EEI-induced quantum correction (the Coulomb correction) to conductivity is:[35–37]

$$\Delta\sigma_T^I = -\frac{e^2}{2\pi^2\hbar}\lambda_T^D \ln\frac{kT\tau}{\hbar}. \tag{7}$$

For a two-dimensional system in a perpendicular magnetic field the WL-induced variation of conductivity can be described as:[38]

$$\Delta\sigma_H^L = \frac{e^2}{2\pi^2\hbar}\left[\frac{3}{2}f_2\left(\frac{4EHD}{\hbar c}\tau_\varphi^*\right) - \frac{1}{2}f_2\left(\frac{4eHD}{\hbar C}\tau_\varphi\right)\right], \tag{8}$$

where $f_2(x) = \ln x + \psi(1/2 + 1/x)$, $\psi$ is the logarithmic derivative of the $\Gamma$ function, and $D$ is the electron diffusion coefficient. The $f_2(x)$ function has the following asymptotic forms: $x^2/24$ at $x \ll 1$ and $\ln x + \psi(1/2)$ at $x \gg 1$. As follows from Eq. (8), magnetoresistance should be negative at $\tau_{so} \gg \tau_{\varphi 0}$ (weak SOI) and positive at $\tau_{so} \ll \tau_{\varphi 0}$ (strong SOI). To compare the experimental magnetic-field variation of the resistance with Eq. (8) for $\Delta\sigma$, the relation $-\Delta\sigma(H) = [R(H) - R(0)]/R(H)R_\square(0)$ is used, which can be applied to resistance when the correction is small.

The EEI-induced magnetic-field variation of conductivity in a diffusion channel can be described as:[40]

$$\Delta\sigma_H^D = -\frac{e^2}{2\pi^2\hbar}\lambda_H^D g_2(h), \tag{9}$$

where $h = g\mu_B H/kT$, $g$ is the Landé factor of conduction electrons, $\mu_B$ is the Bohr magneton, and the function $g_2(h)$ has the asymptotic limits: $0.084h^2$ at $h \ll 1$ and $\ln(h/1.3)$ at $h \gg 1$. On electron repulsion, the quantum correction [Eq. (9)] ensures positive MR.

The EEI-induced quantum correction in the Cooper channel is:[38]

$$\Delta\sigma_H^C = -\frac{e^2}{2\pi^2\hbar}\lambda_H^C \varphi_2(\alpha), \tag{10}$$

where $\alpha = 2eDH/\pi ckT$, and the function $\varphi_2(\alpha)$ has asymptotic limits: $0.3\alpha^2$ at $\alpha \ll 1$ and $\ln\alpha$ at $\alpha \gg 1$. The corrections [Eqs. (9) and (10)] usually appear in quite strong magnetic fields $H \gg \pi kT/g\mu_B, \pi ckT/2eD$.

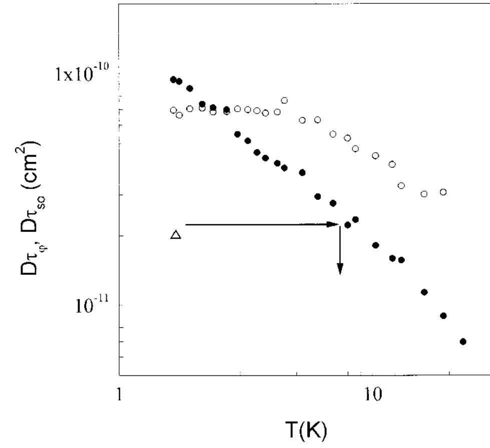


FIG. 5. Temperature dependencies of $D\tau_\varphi$ (●) and $D\tau_{so}$ (○) for sample A obtained from a measurement of magnetic-field dependencies of the resistance at small currents (10 $\mu$A). The symbol △ shows $D\tau_\varphi$ at 1.67 K and 120 $\mu$A, and arrows indicate the method of estimating the electron temperature during electron overheating.

Proceeding from the above relationships, we have analyzed the temperature and magnetic field dependencies of resistance in samples A, B, and C. Assuming that MR is influenced by the WL effect, we employed a computer procedure to fit the theoretical function Eq. (8) and the experimental dependencies and thus obtained the values of $D\tau_\varphi$, $D\tau_\varphi^*$ and $D\tau_{so}$, respectively, at various temperatures. The temperature variations of $D\tau_\varphi$ and $D\tau_{so}$ for sample A are illustrated in Fig. 5. A similar picture is observed for samples B and C. In addition to Eq. (8), the fitting involved a term of the $H^2$ form. This term was practically infinitesimal above 5 K, but below 5 K its amplitude increased by the $T^{-2}$ law. Even at the lowest temperature (1.6 K) the relative contribution of this term to MR was much smaller than that of the WL correction. The term, because of its smallness, could not influence appreciably the calculation of $D\tau_\varphi$ and $D\tau_{so}$ from the MR curves. Its presence indicates that MR is influenced not only by WL corrections but also by the quantum corrections related to EEI [Eqs. (9) and (10)]. Indeed, in quite weak magnetic fields these corrections have the functional form $\propto H^2T^{-2}$. In the case of the quantum correction [Eq. (10)], the analysis of this term gives an unrealistically small value $\lambda_H^C \sim 5\times10^{-5}$; in the case of diffusion correction [Eq. (9)], it gives $g^2\lambda_H^D \sim 3$, which seems reasonable if we assume that $g > 2$ is typical for Sb atoms.

It is seen in Fig. 5 that $D\tau_\varphi$ decreases with rising temperature, approximately following the law $(D\tau_\varphi)^{-1} \propto T^P$, where $p$ is close to unity. This dependence of $\tau_\varphi$ can be attributed to electron-electron scattering in a disordered 2D system.[39,41] The $D\tau_{so}$ values are constant in the low-temperature region; at about 10 K, however, they decrease weakly, which may be due to the contribution of electron-phonon scattering to spin-orbit processes. The remarkable feature in Fig. 5 is the intersection of the $D\tau_\varphi(T)$ dependence with the low-temperature values of $D\tau_{so}$. This implies that to the left of the intersection temperature the spin-orbit interaction is weak, but it is strong at higher temperatures. In the case of strong SOI, the WL-induced correction leads to a

negative MR, which is observed on the samples studied [Fig. 2(a)]. As the sign in the inequality $\tau_{so} > \tau_\varphi$ reverses at low temperatures ($T < 3$ K), a region of positive MR appears in the MR curves of sample A [Fig. 2(a) curve 1]. For samples B and C the interception does not produce any effect, and only negative MR was observed at all temperatures. The $D\tau_\varphi$ and $D\tau_{so}$ values are lower for samples B and C than for sample A, but the difference is mainly due to the changed diffusion coefficient $D$.

To find the time of phase and spin-orbit relaxation in the samples, it is necessary to estimate $D$. For this purpose we used the relaxation $D = (v_F^2 \tau)/2$, in which the time of elastic electron scattering $\tau$ was found from the conductivity $\sigma = ne^2\tau/m$. The Fermi velocities $v_F$ in the $\delta$ layer were calculated from the Hall concentration of electrons, $n$, using the relation $v_F = h(2\pi\hbar^2 n)^{1/2}/m$ for a 2D system. The calculated diffusion coefficients $D$ are 90, 80, and 20 $\mathrm{cm^2\,s^{-1}}$ for samples A, B, and C, respectively. With these values of $D, \tau_{so}$ is within $0.9\times10^{-12}$–$2.4\times10^{-12}$ s, and the characteristic time $\tau_\varphi$, which is assumed to be identical with the electron-electron scattering time $\tau_{ee}$, varies from $\sim 1.5 \times 10^{-12}$ s at the lowest temperature (1.67 K) to $\sim 1.5 \times 10^{-13}$ s at 10 K.

The analysis of $R(T)$ for samples A, B, and C permitted separation of the contributions from the WL equation (6) and Coulombic equation (7) corrections. The contributions can be separated in two ways. (i) Two $R(T)$ dependencies are measured at zero and a strong magnetic field (2.17T in our case). The magnetic field suppresses the WL effect, since the electron wave function acquires an additional phase, which disturbs electron interference. From the measurement in the magnetic field we can derive the Coulombic correction, and the WL-induced correction is found as the difference between the dependencies $-\Delta\sigma(\ln T)$ taken in the magnetic field and in its absence. (ii) Using $\tau_\varphi$ and $\tau_{so}$ obtained from the analysis of MR, the WL-induced correction can be calculated by Eq. (6). This calculation is less reliable, but its results agree with the values derived by the first method within permissible error. The quantum corrections related to the WL and EEI effects turn out to contribute practically equally to the temperature dependence of the samples studied. In the $-\Delta\sigma$ vs $\ln T$ coordinates the Coulombic correction is described by a linear dependence exhibiting a 3% increase in the resistance with the temperature lowering from 10 to 1.67 K. The WL-induced correction for samples B, C, and A at $T > 3$ K also causes a linear increase in the resistance with lowering temperature because $\tau_{so} > \tau_\varphi$. For sample A at $T < 3$ K the inequality becomes $\tau_{so} < \tau_\varphi$; as a result the linearity of $-\Delta\sigma(\ln T)$ is disturbed and a bending is observed.

The EEI constant $\lambda_T^D$ appearing in Eq. (7) can be found from the temperature dependence of the Coulombic correction. The calculated $\lambda_T^D$ values are given in Table I. It is seen that at high electron densities in the $\delta$ layer, the parameter $\lambda_T^D$ is close to unity and decreases with the decrease in electron density. The interaction constant $\lambda_T^D$ can be written in terms of the universal constant $F$, which is an angle-averaged amplitude of the electron interaction with a small transferred momentum.[39,41] With a strong SOI in the magnetic field, the constant $\lambda_T^D$ becomes

$$\lambda_1^D = \begin{cases} 1 - 3F/4, & H < H_0^D \quad (11a) \\ 1 - F/4, & H > H_0^D, \quad (11b) \end{cases}$$

where $H_0^D = \pi kT/g\mu_B$. The $F$ values found from Eq. (11a) are given in Table I. The increase in $F$ with a decreasing electron concentration corresponds to weaker screening in the electron system. In general, screening in a 2D system is less efficient than in a 3D one because the electric field exists in the whole space and the screening electrons can move only in a certain plane. The concentration dependence $F(n)$ can be explained using the relationship for a true 2D system[39] allowing for the specific features of screening in this case,

$$F = \frac{1}{\pi}\frac{1}{(x^2-1)^{1/2}} \ln \frac{x + (x^2-1)^{1/2}}{x - (x^2-1)^{1/2}}, \qquad (12)$$

where $x = 2k_F/\kappa_2$ ($\kappa_2$ is the inverse screening length). Since in a 2D case $k_F = (2\pi n)^{1/2}$, $\kappa_2 = 2\pi e^2 \nu$, and the density of states $\nu = m/\pi\hbar^2$, the parameter $x$ in Eq. (12) depends on the concentration as $n^{1/2}$. In Eq. (12) $x$ decreases inversely with $F$. The numerical $F$ values obtained from the above formulas qualitatively support the observed increase in $F$ with a decreasing concentration of 2D electrons, although it is lower than the value calculated from Eq. (12).

## V. ELECTRON-PHONON RELAXATION

The effect of electron overheating[34,42] can be used to find the electron-phonon relaxation time $\tau_{ep}$. Under electron overheating by the electric field, the transfer of excess energy from the electrons to the lattice is dependent on the time of the electron-phonon energy relaxation. The advantage of this method is that $\tau_{ep}$ can be estimated in the temperature interval where electron-electron scattering is predominant among the inelastic processes of relaxation.

In the electric field $E$ electrons acquire additional energy $\Delta\varepsilon = eE(D\tau_{ep})^{1/2}$, where $(D\tau_{ep})^{1/2}$ is the diffusion length. The transfer of the excess energy from the electrons to the phonon system is controlled by the time $\tau_{ep}$. If the condition $\tau_{ee} < \tau_{esc} < \tau_{ep}$ (where $\tau_{esc}$ is the time of the thermal phonon escape) is met, the electron temperature $T_e$ exceeds the phonon $T_{ph}$. They are related as:[43]

$$(kT_e)^2 = (kT_{ph})^2 + \frac{\pi}{6}(eE)^2 D\tau_{ep}. \qquad (13)$$

When the electron gas overheating $\Delta T = T_e - T_{ep}$ is known, $D\tau_{ep}$ can be found from Eq. (13). The electron temperature can be estimated using the $D\tau_\varphi$ data obtained from the magnetic-field variations of the WL-induced quantum correction [Eq. (8)]. Two types of dependencies should be plotted: (i) $D\tau_\varphi(T)$ at varying temperatures, and a certain lowest current (the equilibrium dependence, Fig. 5), and (ii) $D\tau_\varphi(E)$ at certain temperatures and varying currents. In the latter case the decrease in $D\tau_\varphi$, with growing $E$, is due to the

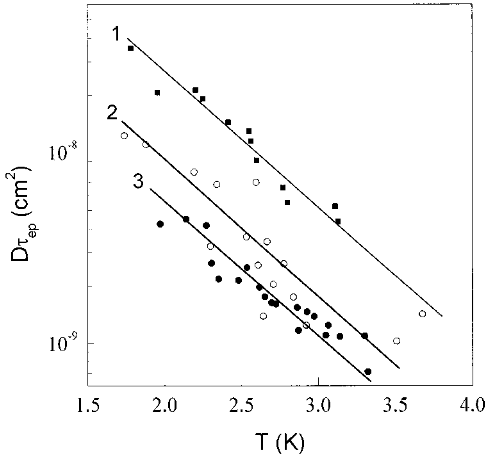


FIG. 6. $D\tau_{\mathrm{ep}}(T)$ dependence for samples A (1), B (2), and C (3).

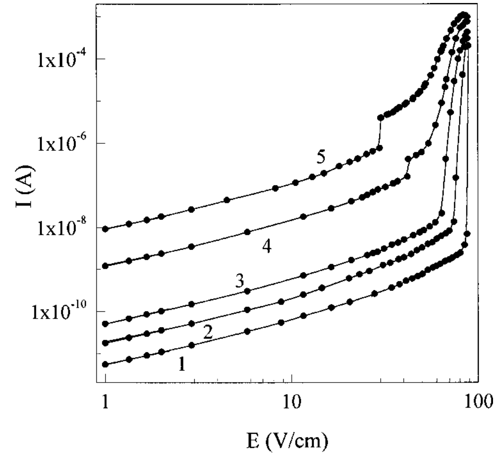


FIG. 7. $I$-$V$ curves for sample E at various temperatures K: 10 (1), 14 (2), 16.6 (3), 18.9 (4), and 20.4 (5).

rising electron temperature $T_e$, which can be found from the equilibrium dependence $D\tau_\varphi(T)$. An example of such estimation is illustrated in Fig. 5. The phonon temperature is set equal to the crystal temperature. The advantage of Eq. (13) is that it includes [like Eq. (8) for the WL-induced quantum correction] the diffusion coefficient $D$ as the only characteristic of the system under investigation.

For samples A, B, and C, the $D\tau_{\mathrm{ep}}$ value was calculated in the temperature interval 1.67–4 K, with currents varying from 10 to 120 $\mu$A. The $D\tau_{\mathrm{ep}}(T)$ dependencies plotted for these three samples are shown in Fig. 6. The dependencies can be approximated by the power function of the form $(D\tau_{\mathrm{ep}})^{-1}\propto T^p$, where $p$ is $3.7\pm0.3$. Using the estimated $D$ values, we obtained the characteristic times $\tau_{\mathrm{ep}}$ of the electron-phonon relaxation within $1.5\times10^{-10}-5.9\times10^{-9}$ s at 1.7 K and $1.17\times10^{-11}-4.4\times10^{-11}$ s at 4 K. Note that for samples A and B, the elastic time $\tau$ is about $3\times10^{-15}$ s. Thus, below 4 K the relaxation times form the sequence $\tau \ll \tau_{\mathrm{ee}} \leq \tau_{\mathrm{so}} \ll \tau_{\mathrm{ep}}$.

For electron-phonon relaxation in pure metal systems the $\tau_{\mathrm{ep}}^{-1}\propto T^3$ dependence is known, which holds for weak disorder[44] when $q_Tl\gg1$, where $q_T$ is the wave vector of the thermal phonon ($q_T=kT/\hbar s$, $s$ being the velocity of sound), $l$ is the electron mean free path. This form of the $\tau_{\mathrm{ep}}^{-1}(T)$ dependence is due to the increasing number of thermal phonons at rising temperature. In the case of strong disorder ($q_Tl<1$), the temperature dependence of the electron-phonon relaxation time assumes the form $\tau_{\mathrm{ep}}^{-1}\propto lT^4$,[45,46] which suggests a weakening of the electron-phonon interaction when the electron mean free path is shorter then the thermal phonon wavelength. In the $\delta$ layer, the electrons are two dimensional, since they occupy quantum levels in a certain potential well and have momentum vectors lying on in-plane cross sections in reciprocal space. The phonons interacting with electrons are, however, three dimensional, and their interaction with electrons involves the component of the phonon wave vector out of the 2D plane. The kinetic characteristics of 2D and 3D electrons differ only in numerical factor[47,48] since 2D electrons have a lower possibility of changing their moment. We may assume that the functional dependencies $\tau_{\mathrm{ep}}^{-1}(T)$ at $q_Tl>1$ and $q_Tl<1$ are similar in character for 2D and 3D systems. The $(D\tau_{\mathrm{ep}})^{-1}\propto T^p$ dependence with $p$ close to 4 is most likely due to disorder in the $\delta$ layer and the short electron mean free path. The estimated $q_Tl$ supports this conclusion: it turns out that $q_Tl<1$ below 4 K.

## VI. NONLINEAR EFFECTS IN THE CASE OF HOPPING CONDUCTIVITY

Samples D and E have nonlinear conductivity. The $I$-$V$ characteristics (IVC's) of sample D at different temperatures are shown in Fig. 7. In addition to nonlinearity, they exhibit a sharp jump in current at high voltages. At 10 K and the electric field $E_B\approx90$ V/cm, the current jumps up by six orders of magnitude. As the temperature rises, the starting voltage of the jump decreases and the jump itself is voltage smeared. The jump can be classified as an impurity breakdown caused by ionization of impurities and the introduction of charge carriers to the conduction band. Above 16 K the main jump is preceded with a smaller-amplitude jump, which may be due to filling the quantum states below the bottom of the conduction band.

Variations of the hopping conductivity in the region that obeys Mott's law, [Eq. (3)] in a strong electric field are discussed in Refs. 49–53. In the region of very strong electric fields $E>kT/E_A$, the dependence

$$J(E)\propto\exp(-E_0/E)^{1/4}, \qquad (14)$$

is expected,[49] where $E_0\approx kT_0/ea$. The theory of non-Ohmic hopping conductivity in moderate electric fields ($E<kT/ea$) was developed in Ref. 53, which is based on percolation theory and allows for variation of the distribution function at the initial and final localized states. Reference 53 predicted a departure from linearity in the field at

$$E_c=kT/eL_0, \qquad (15)$$

where $L_0$ is the characteristic size of the critical percolation subnetwork of the states over which jumps are realized. It can be represented in terms of the percolation threshold

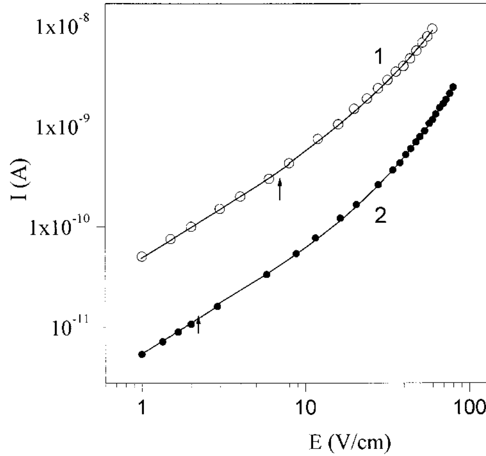


FIG. 8. $I$-$V$ curves for sample E at 10 K (1) and sample D at 4.2 K (2):—fitting of Eq. (16); ●●●, experimental results; arrows show the change from a linear dependence to a nonlinear dependence $I(E)$.

$\xi_c L_0 \approx r\xi_c^{\nu}$, where $r$ is the mean jump length in the region in which Mott's law [Eq. (3)] is operative [$r\approx a(T_0/T)^{1/4}$ (Ref. 25)], $\nu$ is the correlation radius index, which is 0.9 and 1.3 for 3D and 2D cases respectively.[54] Since $(T_0/T)^{1/4}\equiv\xi_c$,[54] the parameter $L_0$ can be represented as $L_0\approx a\xi_c^{1+\nu}$. At $E > E_c$ it is expected[53] that

$$j(E,T)=\sigma(T)E_c\exp(eEL_0/kT)^{1/1+\nu}. \tag{16}$$

Like Eq. (15), this dependence holds good for hopping-type conductivity both at constant and decreasing activation energy: only the $\sigma(T)$ dependence and the parameters $\xi_c$ and $L_0$ must have the corresponding form.[54]

The theory developed in Ref. 53 describes well the IVC nonlinearity for samples D and E, and provides good quantitative agreement of the characteristic fields of the nonlinearity onset $E_c$, the impurity breakdown $E_B$ and the size $L_0$ of the critical subnetwork of donor states. Examples of the computer fitting (solid curves) of the dependence [Eq. (16)] and the experimental results for the nonlinear IVC part (up to the breakdown voltage) for samples D (4.2 K) and E (10 K) are illustrated in Fig. 8. Taking $E_c\approx 2$ V/cm for sample E (see Fig. 8), we obtain $L_0\approx 4.3\times 10^{-4}$ cm, according to Eq. (15). For sample D these values are $E_c\approx 8$ V/cm and $L_0 \approx 4.5\times 10^{-5}$ cm, respectively. Using the calculated $L_0$ values, the electric field $E_B$ of the breakdown can be found from $eE_BL_0\approx\varepsilon_0$ ($\varepsilon_0$ is the energy of the ground Sb impurity state in silicon), which we compare to the experimental value $\varepsilon_1 \approx 44$ meV. The estimate $E_B\approx 100$ V/cm obtained by this method is close to the corresponding experimental result and exceeds it only by $\sim$10%. On the other hand, $L_0$ can be estimated from the temperature dependence of resistance. From Fig. 1(c) we can obtain $T_0\approx 25\times 10^3$ K for sample D, and since $L_0\approx a\xi_c^{1+\nu}$, where $\xi_c=(T_0/T)^{1/3}$, then we obtain $\xi_c\approx 15$ and $L_0\approx 5.5\times 10^{-5}$ cm at 10 K, which is in good agreement with the above $L_0$.

## VII. CONCLUSIONS

The studies of the electrical properties of Si single crystals with the $\delta\langle\mathrm{Sb}\rangle$ layer of various sheet concentrations $N_D$ of Sb atoms ($5\times 10^{12}$–$3\times 10^{14}$ cm$^{-2}$) have provided detailed information about the low-temperature features of the electron transport in this system. The findings are as follows.

(1) At $N_D$ below $\sim 3\cdot 10^{13}$ cm$^{-2}$ a metal-insulator transition occurs, which is accompanied by a change from the metal-type conductivity of the $\delta\langle\mathrm{Sb}\rangle$ layer to hopping conductivity in a 2D system.

(2) As the temperature is increased, the impurity conduction in the $\delta$ layer changes to a higher conductivity in the Si crystal due to activation of the electrons to the conduction band. The change of impurity conductivity to band conductivity with increasing $N_D$ occurs at a progressively higher temperature.

(3) With the metallic conductivity in the $\delta$ layer, the temperature and magnetic-field variations of the samples at low temperatures are dependent on the quantum corrections related to the effects of weak electron localization and the electron-electron interaction. The analysis of the magnetic field dependencies of resistance controlled mainly by the WL-induced quantum correction permitted us to find the temperature dependence of the phase-breaking time $\tau_\varphi \propto T^{-1}$, identified as the time of the electron-electron interaction.

(4) The separation of the WL and EEI contributions in the temperature dependence of resistance permitted estimation of the EEI constant $\lambda_T^D$ for samples of different densities $N_D$. It is found that $\lambda_T^D$ decreases with $N_D$ because screening becomes weaker with lowering densities $n$ of 2D electrons.

(5) The effect of electron overheating was used to find the temperature dependence of the electron-phonon relaxation time $\tau_{\mathrm{ep}}$, $\tau_{\mathrm{ep}}\propto T^p$, where $p\approx 3.7\pm 0.3$, which should be interpreted as the manifestation of the electron-phonon scattering at strong disorder and high frequency of the elastic scattering $\tau^{-1}$ in the $\delta$ layer. Below 4 K the relaxation times follow the hierarchy $\tau \ll \tau_{\mathrm{ee}} \leqslant \tau_{\mathrm{so}} \ll \tau_{\mathrm{ep}}$.

(6) With the hopping-type conductivity, the current-voltage characteristics become nonlinear at quite low voltages (much lower than the impurity breakdown voltage). The IVC nonlinearity is well described by Shklovskii's theory of non-Ohmic hopping conductivity.[53] The theory gives good quantitative agreement of the characteristic fields $E_c$ in which nonlinearity appears, the impurity breakdown $E_B$, and the size $L_0$ of the critical percolation subnetwork of donor states in which jumps are realized.

---

*On leave from Department of Physics, Kirikkale University, 71450 Kirikkale, Turkey.

†On leave from Institute for Radiophysics and Electronics, National Academy of Sciences of Ukraine, 310085 Kharkov, Ukraine.

[1] A. Ya Shik, Fiz. Tekh. Poluprovod. **26**, 1161 (1992) [Sov. Phys. Semicond. **26**, 649 (1992)].

[2] A. Zrener, H. Reisinger, F. Koch, K. Ploog, and J. C. Maan, Phys. Rev. B **33**, 5607 (1986).

[3] E. F. Schubert, J. E. Cunningham, and W. T. Tsang, Solid State Commun. **63**, 591 (1987).

[4] P. M. Koenraad, B. F. A. van Hest, F. A. P. Blom, R. van Dalen, M. Leys, J. A. A. J. Perenboom, and J. H. Wolter, Physica B **177**, 485 (1992).

[5] P. M. Koenraad, A. C. L. Heessels, F. A. P. Blom, J. A. A. J. Perenboom, and J. H. Wolter, Physica B **184**, 221 (1993).

[6] G. M. Gusev, Z. D. Kvon, D. I. Lubyshev, V. P. Migal', V. N. Ovsiuk, V. V. Preobragenskii, and S. I. Stenin, Fiz. Tverd. Tela (Leningrad) **30**, 3148 (1998) [Sov. Phys. Solid State **30**, 1804 (1988)].

[7] G. M. Gusev, Z. D. Kvon, D. I. Lubyshev, V. P. Migal', and A. G. Pogosov, Fiz. Tekh. Poluprovodn. **25**, 601 (1991) [Sov. Phys. Semicond. **25**, 364 (1991)].

[8] I. A. Panaev, S. A. Studenikin, D. I. Lubyshev, and V. P. Migal', Semicond. Sci. Technol. **8**, 1822 (1993).

[9] A. A. van Gorkum, K. Nakagawa, and Y. Shiraki, J. Appl. Phys. **65**, 2485 (1989).

[10] N. L. Mattey, M. Hopkinson, R. F. Houghton, M. G. Dowsett, D. S. McPhail, T. E. Whall, E. H. C. Parker, R. G. Booker, and J. Whitehurst, Thin Solid Films **184**, 15 (1990).

[11] A. R. Powell, R. A. A. Kubiak, T. E. Whall, and D. K. Bowen, J. Phys. D **23**, 1745 (1990).

[12] H. P. Zeindl, T. Wegehaupt, I. Eisele, H. Oppolzer, H. Reisinger, G. Tempel, and F. Koch, Appl. Phys. Lett. **50**, 1164 (1987).

[13] L. Ioviatti, Phys. Rev. B **41**, 8340 (1990).

[14] O. Mezrin and A. Shik, Superlattices Microstruct. **10**, 107 (1991).

[15] A. Zrenner, F. Koch, and K. Ploog, Surf. Sci. **196**, 671 (1988).

[16] L. R. Gonzalez, J. Krupski, and T. Szwacka, Phys. Rev. B **49**, 11 111 (1994).

[17] Guo-Qiang Hai, N. Stuart, and F. M. Peeters, Phys. Rev. B **52**, 8363 (1995).

[18] A. B. Henrigues, Phys. Rev. B **53**, 16 365 (1996).

[19] N. L. Mattey, T. E. Whall, R. A. Kubiak, and M. J. Kearney, Semicond. Sci. Technol. **7**, 604 (1992).

[20] T. Ando, A. B. Fowler, and F. Stern, Rev. Mod. Phys. **54**, 437 (1982).

[21] F. Stern, Phys. Rev. B **5**, 4891 (1972).

[22] J. J. Harris, R. Murray, and C. T. Foxon, Semicond. Sci. Technol. **8**, 31 (1993).

[23] W. T. Masselink, Appl. Phys. Lett. **59**, 694 (1991).

[24] S. Iwabuchi and Y. Nagaoka, J. Phys. Soc. Jpn. **58**, 1325 (1989).

[25] B. I. Shklovskii and A. L. Efros, *Electronic Properties of Doped Semiconductors* (Springer, New York, 1984).

[26] N. F. Mott, J. Non-Cryst. Solids **1**, 1 (1968).

[27] A. S. Skal and B. I. Shklovskii, Fiz. Tverd. Tela (Leningrad) **16**, 1820 (1974) [Sov. Phys. Solid State **16**, 1190 (1975)].

[28] W. Brenig, G. H. Dohler, and H. Heyszenau, Philos. Mag. **27**, 1083 (1973); Qiu-Yi Ye, A. Zrenner, F. Koch, and K. Ploog, Semicond. Sci. Technol. **4**, 500 (1989).

[29] Qiu-Yi Ye, B. I. Shklovskii, A. Zrenner, F. Koch, and K. Ploog, Phys. Rev. B **41**, 8477 (1990).

[30] M. E. Raikh, J. Czingon, Qiu-Yi Ye, and F. Koch, Phys. Rev. B **45**, 6015 (1992).

[31] B. I. Shklovskii, Zh. Eksp. Teor. Fiz. **61**, 2033 (1971) [Sov. Phys. JETP **34**, 1084 (1972)].

[32] B. I. Shklovskii, Fiz. Tverd. Tela (Leningrad) **8**, 416 (1966) [Sov. Phys. Solid State **8**, 331 (1966)].

[33] E. Abrahams, P. W. Anderson, D. C. Licciardello, and T. V. Ramakrishnan, Phys. Rev. Lett. **42**, 673 (1979).

[34] P. W. Anderson, E. Abrahams, and T. V. Ramakrishnan, Phys. Rev. Lett. **43**, 718 (1979).

[35] B. L. Altshuler and A. G. Aronov, Pis'ma Zh. Eksp. Teor. Fiz. **30**, 514 (1979) [JETP **30**, 482 (1979)]; Zh. Eksp. Teor. Fiz. **77**, 2028 (1979) [Sov. Phys. JETP **50**, 968 (1979)].

[36] B. L. Altshuler, D. E. Khmel'nitskii, A. I. Larkin, and P. A. Lee, Phys. Rev. B **22**, 5142 (1980).

[37] B. L. Altshuler, A. G. Aronov, and P. A. Lee, Phys. Rev. Lett. **44**, 1288 (1980).

[38] B. L. Altshuler, A. G. Aronov, A. I. Larkin, and D. E. Khmel'nitskii, Zh. Eksp. Teor. Fiz. **81**, 768 (1981) [Sov. Phys. JETP **54**, 411 (1981)].

[39] B. L. Altshuler and A. G. Aronov, in *Electron-Electron Interaction in Disordered Systems*, Modern Problems in Condensed Matter Science, Vol. 10, edited by A. L. Efros and M. P. Pollak (North-Holland, Amsterdam, 1985), p. 1.

[40] P. A. Lee and P. V. Ramakrishnan, Rev. Mod. Phys. **53**, 287 (1985).

[41] B. L. Altshuler, A. G. Aronov, M. E. Gershenzon, and Yu. V. Sharvin, Sov. Sci. Rev., Sect. A **9**, 223 (1987).

[42] V. A. Shklovskii, J. Low Temp. Phys. **41**, 375 (1980).

[43] S. Hershfield and V. Ambegaokar, Phys. Rev. B **34**, 2147 (1986).

[44] J. Rammer and A. Schmid, Phys. Rev. B **34**, 1352 (1986).

[45] A. Schmid, Z. Phys. **259**, 421 (1973).

[46] M. Yu. Reyzer and A. V. Sergeev, Zh. Eksp. Teor. Fiz. **90**, 1056 (1986) [Sov. Phys. JETP **63**, 616 (1986)].

[47] V. Karpus, Fiz. Tekh. Poluprovodn. **20**, 12 (1986) [Sov. Phys. Semicond. **20**, 6 (1986)]; **22**, 439 (1988) [ **22**, 268 (1988)].

[48] P. J. Price, Ann. Phys. (N.Y.) **133**, 217 (1981).

[49] B. I. Shklovskii, Fiz. Tekh. Poluprovodn. **6**, 2335 (1972) [Sov. Phys. Semicond. **6**, 1964 (1972)].

[50] R. M. Hill, Philos. Mag. **24**, 1307 (1971).

[51] H. Botger and V. V. Bryksin, Phys. Status Solidi B **67**, 583 (1975); **68**, 285 (1975).

[52] M. Pollak and I. Riess, J. Phys. C **9**, 2339 (1976).

[53] B. I. Shklovskii, Fiz. Tekh. Poluprovodn. **10**, 1440 (1976) [Sov. Phys. Semicond. **10**, 855 (1976)].

[54] B. I. Shklovskii and A. L. Efros, Usp. Fiz. Nauk. **117**, 401 (1975) [Sov. Phys. Usp. **18**, 845 (1975)].